Structural determination of a 5-*O*-methyl-deaminated neuraminic acid (Kdn)-containing polysaccharide isolated from *Sinorhizobium fredii*

Antonio M. GIL-SERRANO*[1], Miguel A. RODRÍGUEZ-CARVAJAL*, Pilar TEJERO-MATEO*, José L. ESPARTERO†, Jane THOMAS-OATES‡, José E. RUIZ-SAINZ§ and Ana M. BUENDÍA-CLAVERÍA§

*Departamento de Química Orgánica, Facultad de Química, Universidad de Sevilla, 41071-Sevilla, Spain, †Departamento de Química Orgánica y Farmacéutica, Facultad de Farmacia, Universidad de Sevilla, 41071-Sevilla, Spain, ‡Department of Mass Spectrometry, Bijvoet Center for Biomolecular Research, Utrecht University, Sorbonnelaan 16, 3584 CA Utrecht, The Netherlands, and §Departamento de Microbiología, Facultad de Biología, Universidad de Sevilla, 41071-Sevilla, Spain

The structure of a polysaccharide from *Sinorhizobium fredii* SVQ293, a thiamine auxotrophic mutant of *S. fredii* HH103, has been determined. This polysaccharide was isolated following the protocol for lipopolysaccharide extraction. On the basis of monosaccharide analysis, methylation analysis, fast atom bombardment MS, collision-induced dissociation tandem MS, one-dimensional ^{1}H and ^{13}C NMR and two-dimensional NMR experiments, the structure was shown to consist of the following trisaccharide repeating unit → 2)-α-D-Gal*p*-(1 → 2)-β-D-Rib*f*-(1 → 9)-α-5-*O*-Me-Kdn*p*-(2 → , in which Kdn stands for deaminated neuraminic acid; 25 % of the Kdn residues are not methylated. The structure of this polysaccharide is novel and this is the first report of the presence of Kdn in a rhizobial polysaccharide, as well as being the first structure described containing 5-*O*-Me-Kdn. This Kdn-containing polysaccharide is not present in the wild-type strain HH103, which produces a 3-deoxy-D-*manno*-2-octulosonic acid (Kdo)-rich polysaccharide. We conclude that it is likely that the appearance of this new Kdn-containing polysaccharide is a consequence of the mutation.

INTRODUCTION

Rhizobium and *Bradyrhizobium* species are Gram-negative bacteria that are able to induce the formation of a nitrogen-fixing organ (nodule) on the roots of leguminous plants. This symbiotic bacterium–plant interaction results in the inclusion of highly differentiated bacterial cells (bacteroids) in host plant nodule cells, where they perform the reduction of atmospheric nitrogen to ammonia, which is then utilized by the host plant. The development of legume nodules is controlled largely by reciprocal signal exchange between the symbiotic partners. Legume roots secrete specific flavonoids or isoflavonoids that induce the transcription of many bacterial genes that direct the early steps of this interaction [1]. Many of these genes are involved in the synthesis and secretion of lipo-chitin oligosaccharides, known as LCOs or Nod factors, that trigger root hair deformations and cell division in susceptible regions of the root [2,3]. For the bacteria to infect and for the nodules to differentiate normally, other bacterial determinants besides the LCOs are required. These determinants include certain polysaccharides that are present in the bacterial cell wall: β-glucans, acidic exopolysaccharides, capsular polysaccharides and lipopolysaccharides (LPS) [4,5].

The cell wall of Gram-negative bacteria consists of the cytoplasmic membrane (inner membrane) and the outer membrane, with a periplasmic space between the two bacterial membranes. The outer membrane is attached via lipoproteins to the peptidoglycan layer and consists of an asymmetric lipid bilayer; the outer leaflet is formed by the lipid tails of LPS molecules and the inner leaflet is composed of phospholipids and lipoproteins. LPS molecules comprise three major moieties: the lipid A membrane anchor, a core oligosaccharide linked to the lipid A via 3-deoxy-D-*manno*-2-octulosonic acid (Kdo), and an antigenic polysaccharide (O-antigen). The bacterial cell surface is often covered with an extracellular layer of polysaccharide (capsular polysaccharides), commonly termed the capsule. The extracellular matrix of the bacterium consists of acidic exopolysaccharide, which is released into the cell's milieu as extracellular slime. Numerous reports have shown that the different rhizobial polysaccharides have important roles in the interaction between the bacteria and their legume hosts.

Reuhs et al. [6] have reported that β-glucans, acidic exopolysaccharides, capsular polysaccharides and LPS are not the only cell-associated polysaccharides produced by *Rhizobium*. They described a Kdo-containing polysaccharide (called Kdops) that is structurally analogous to the constituents of one subgroup of K antigens (capsular polysaccharides) produced by *Escherichia coli*. [7]. We have shown that *Sinorhizobium fredii* HH103 also produces a Kdo-containing polysaccharide that yields a ^{1}H-NMR spectrum that is very similar to that described for the Kdops of *Rhizobium meliloti* AK631 [6] (results not shown). However, when the standard protocols for LPS purification were applied to a thiamine auxotrophic mutant (strain SVQ293) derivative of HH103, two fractions were identified on gel-permeation chromatography of the phenol/water extract. The minor polysaccharide fraction had a sugar and fatty acid composition typical of an LPS; the major polysaccharide fraction was a new type of capsular polysaccharide, a deaminated neuraminic acid (Kdn)-rich polysaccharide that is not present in the wild-type strain HH103 and is analogous to the Kdops described by Reuhs [6]. Because this new Kdn-rich polysaccharide is apparently not present in the wild-type strain HH103, we

Abbreviations used: 1D, one-dimensional; 2D, two-dimensional; CID-MS, collision-induced dissociation MS; DBF, double-band-filtered; DQF, double-quantum-filtered; EI-MS, electron-impact MS; FAB, fast atom bombardment; HSQC, ^{1}H-detection mode via single-quantum coherence; Kdn, deaminated neuraminic acid; Kdo, 3-deoxy-D-*manno*-2-octulosonic acid; Kdops, Kdo-containing polysaccharide; LPS, lipopolysaccharide(s); TY medium, bacto-tryptone yeast medium.

[1] To whom correspondence should be addressed (e-mail agil@cica.es).

conclude that the appearance of this new polysaccharide is a consequence of the mutation affecting strain SVQ293.

EXPERIMENTAL

General methods

GLC–MS was performed with a Kratos MS80RFA instrument fitted with a CP-Sil5 CB column (25 m × 0.32 mm). The temperature programme for separating the trimethylsilylated methyl glycosides was isothermal at 140 °C for 2 min followed by an 8 °C/min gradient up to 250 °C, whereas that for the trimethylsilylated (+)-2-butyl analogues was isothermal at 130 °C followed by a 2 °C/min gradient up to 250 °C. The protocol for the partly methylated alditol acetates was isothermal at 100 °C for 1 min followed by a 5 °C/min gradient up to 250 °C. The ionization potential was 70 eV. The reduced and methylated trisaccharide was analysed by direct introduction and electron-impact MS (EI-MS).

Bacterial strains and isolation of the polysaccharide

Wild-type *S. fredii* strain HH103 and its SVQ293 derivative were routinely grown at 28 °C in bacto-tryptone yeast (TY) medium as described by Beringer [8]. *E. coli* strains were grown on Luria–Bertani medium [9]. When required, the media were supplemented with the appropriate antibiotics: streptomycin (400 μg/ml), kanamycin (50 μg/ml, or 25 μg/ml for *E. coli*) and nalidixic acid (20 μg/ml). To perform random transposon mutagenesis, plasmid pSUP5011 (carrying transposon Tn5-Mob) was transferred by conjugation from *E. coli* S17-1 to *S. fredii* HH103-1 (a streptomycin-resistant derivative of HH103) as described by Simon [10]. Kanamycin-resistant transconjugants were selected in TY medium supplemented with streptomycin, kanamycin and nalidixic acid. Early-stationary-phase cultures (300 ml, TY medium) of *S. fredii* strains HH-103 and SVQ293 were used to inoculate 30 litres of TY liquid medium supplemented with the antibiotics streptomycin (for HH103) or kanamycin (for SVQ293). After inoculation, cultures were incubated for 3 days at 28 °C. Bacterial cultures were aerated by pumping sterile air through at a flow rate of 50 l/min. After incubation the cells were harvested by low-speed centrifugation. The bacterial pellets were washed with 0.9 % NaCl, freeze-dried and stored in sealed bottles at room temperature. The polysaccharide was extracted from the freeze-dried bacterial cells (5 g) with 100 ml of hot phenol/water mixture (1:1, v/v) [11] and the two phases were separated. The aqueous phase was dialysed against water, concentrated and passed through an IRA 400 Amberlite (AcO^-) anion-exchange resin (30 cm × 1.6 cm) with water as eluent. The eluate was freeze-dried and redissolved in 100 ml of 10 mM $MgSO_4$/50 mM Tris/HCl (pH 7.0); DNase (1 mg) and RNase A (1 mg) were added and the solution was stirred overnight at 5 °C. Proteinase K (10 mg) was added and the solution was shaken for 24 h at 37 °C, dialysed and then freeze-dried. The polysaccharide was chromatographed on Sephacryl S-500 (60 cm × 2.6 cm) with 0.2 M NaCl as eluent; carbohydrates were detected with a refractive index detector and the orcinol/sulphuric acid method [12] on TLC plates. Fractions containing carbohydrates were dialysed and freeze-dried.

SDS/PAGE

Bacterial cultures of *S. fredii* HH103 and SVQ293 were grown on TY medium. For SDS/PAGE the polysaccharide was solubilized from proteinase K-treated cells as described by Köplin et al. [13]. The bacterial pellet was lysed by heating at 100 °C in 125 μl of 60 mM Tris/HCl (pH 6.8)/1 % (w/v) SDS for 5 min and then diluted to 1 ml with the same buffer without SDS. RNase and DNase were added and the solution was incubated at 37 °C for 5 h. Proteinase K was added to a final concentration of 10 μg/ml, and incubation proceeded for a further 24 h. Electrophoresis was performed on a 16.5 % (w/v) polyacrylamide gel with the tricine buffer system described by Lesse et al. [14]. Gels were fixed and silver-stained as described by Kittelberger and Hilbink [15].

Monosaccharide analysis

Monosaccharides were determined after GLC–MS separation of their trimethylsilylated methyl glycosides. The polysaccharide was treated with 0.625 M HCl in methanol at 80 °C for 16 h. 2-Methylpropan-1-ol was added to the mixture, which was then dried under a stream of nitrogen. The methyl glycosides were silylated with pyridine/bis(trimethylsilyl)trifluoroacetamide (1:1, v/v) for 2 h at room temperature [16]. The absolute configurations of the monosaccharides were assigned after GLC–MS analysis of their trimethylsilylated 2-butylglycosides, prepared with (+)-2-butanol and (±)-2-butanol [17] as above.

Methylation

Vacuum-desiccated samples of polysaccharide were dissolved in 50–200 μl of a NaOH/DMSO suspension prepared by vortex-mixing of DMSO and dry, finely ground NaOH pellets. After 1 h at room temperature, 10–50 μl of methyl iodide was added and the solution was kept for 1 h at room temperature with occasional vortex-mixing [18]. Aqueous 10 % (w/v) $Na_2S_2O_3$ was added and the mixture was dialysed against water. The permethylated polysaccharide was further purified by gel-permeation chromatography on Sephadex LH-20 with dichloromethane/ethanol (1:1, v/v) as eluent. Hydrolysis was performed with 1 ml of 88 % (v/v) formic acid for 1 h at 100 °C; the reagent was then evaporated and the residue was redissolved in 1 ml of 2 M trifluoroacetic acid and hydrolysed for 1.5 h at 121 °C. The released methylated monosaccharides were reduced with NaB^2H_4 and acetylated by the method described by Blakeney [19]. For the oligosaccharide, the sample (200 μg) was treated with a 10 μg/μl solution of NaB^2H_4 in 1 M NH_4OH (200 μl) for 4 h at room temperature. The pre-reduced oligosaccharide was methylated as above with C^2H_3I. The methylated sample was extracted with chloroform and then purified by reverse-phase chromatography on a Sep-Pak C_{18} cartridge [20]. One portion was analysed by fast atom bombardment (FAB) MS and by EI-MS. Another portion was further hydrolysed with 2 M trifluoroacetic acid, reduced and acetylated as described for the polysaccharide.

Isolation and purification of trisaccharide repeating unit

The trisaccharide was released from the polysaccharide by autohydrolysis. The polysaccharide (2.4 mg) was treated with water (1 ml) at 60 °C for 3 h and the progress of the reaction was monitored by TLC on Silica Gel 60 developed in butanol/acetic acid/water (2:1:1, by vol.). The hydrolysate was passed through a Sephadex G-50 column (40 cm × 1.6 cm) with 5 % (v/v) ethanol as eluent.

FAB and collision-induced dissociation (CID) tandem MS

The positive-ion FAB mass spectrum of the intact oligosaccharide was obtained by using MS1 of a JEOL JMS-SX/SX102A tandem mass spectrometer operated at + 10 kV accelerating voltage. The FAB gun was operated at 4 kV accelerating voltage with an

emission current of 10 mA and xenon as the bombarding gas. Spectra were scanned at a speed of 30 s for the full mass range specified by the accelerating voltage used, and were recorded and averaged on a Hewlett Packard HP9000 data system running Jeol COMPLEMENT software. Negative-ion CID-MS spectra were recorded with the same machine and an accelerating voltage of -10 kV, with helium as the collision gas in the third field free region collision cell, at a pressure sufficient to decrease the parent ion intensity to one-third of the original. The oligosaccharide was dissolved in 30 μl of water, and 1 μl aliquots of sample solution were loaded into a matrix of glycerol. For the pre-reduced and fully methylated oligosaccharide, FAB mass spectra were obtained in the positive mode by using a Kratos MS80-RFA instrument with a xenon atom beam at an accelerating voltage of 4 kV. The probe was loaded with 1 μl of sample solution in acetone with a matrix of nitrobenzyl alcohol and NaI as the cationizing agent.

NMR spectroscopy

The samples were deuterium-exchanged several times by freeze-drying from ^2H_2O and then examined in solution (3 mg/ml) in 99.98 % ^2H_2O. Spectra were recorded at 303 K on a Bruker AMX500 spectrometer operating at 500.13 MHz (^{1}H) and 125.75 MHz (^{13}C). Chemical shifts are given in p.p.m., with the H^{2}HO signal (4.75 p.p.m.) (^{1}H) and external DMSO (39.5 p.p.m.) (^{13}C) as references. Two-dimensional (2D) homonuclear proton double-quantum filtered (DQF) COSY [21] was performed in the phase-sensitive mode with the Bruker standard pulse sequence. A data matrix of 512×1K points was used to digitize a spectral width of 4500 Hz; 32 scans were used per increment with a delay between scans of 1 s. Before Fourier transformation, zero-filling was used in F_1 to expand the data to $1K \times 1K$. The 2D heteronuclear one-bond proton–carbon correlation experiment [22] was registered in the ^{1}H-detection mode via single-quantum coherence (HSQC). A data matrix of 512×1K points was used to digitize a spectral width of 4500 and 26000 Hz in F_2 and F_1; 128 scans were used per increment with a delay between scans of 1 s and a delay corresponding to a J value of 150 Hz. ^{13}C decoupling was achieved by the GARP scheme. Squared cosine-bell functions were applied in both dimensions and zero-filling was used to expand the data to $1K \times 1K$. This experiment was modified slightly by the implementation of an editing block in the sequence [23]. The pure absorption 2D NOESY experiments were performed with mixing times of 200 ms. Acquisition and data processing were similar to those used for the DQF-COSY.

Selective excitation one-dimensional (1D) experiments were performed by application of the DANTE-Z pulse train ($n = 300$, $\tau = 100$ μs, $\theta = 0.3$ °) [24]. This train was also concatenated with a TOCSY sequence (isotropic mixing time of 120 ms, $\pi/2$ pulse width of 49 μs) [25] to yield the 1D-TOCSY subspectra. The number of accumulated scans was 512, which corresponds to a total acquisition time of 30 min. The 2D homonuclear proton double-band filtered selective correlation experiment (DBF-COSY) [26] was collected by the application of two BURP pulses based on the DANTE-Z scheme [27] ($n = 10$, $\tau = 50$ μs, $\theta = 10$ °). A data matrix of 512×1K points was used to resolve a spectral width of 1500 Hz; 64 scans were used per increment. The H^{2}HO signal was generally presaturated by a low-power pulse (transmitter attenuation, 70 dB) of 1.2 s.

RESULTS

Isolation and purification of the polysaccharide

Random transposon Tn5-Mob mutagenesis was performed on *S. fredii* strain HH103 by using the suicide plasmid pSUP5011. Km-r HH103 transconjugates (8×10^4) were visually screened for the appearance of mutants showing alterations in their colony morphology. One such mutant (named SVQ293) forms a colony producing more slime than its parent strain. To investigate whether the LPS of mutant SVQ293 are altered, crude cell extracts from cultures of wild-type strain HH103 and SVQ293 were analysed by PAGE. In general, PAGE separates the LPS of many rhizobia strains (including *Sinorhizobium* strains) into two mobility classes, LPS II and faster-moving LPS I bands. LPS I comprises lipid A and core oligosaccharide; LPS II comprises lipid A, core, and various forms of O-antigen [28,29]. Figure 1 (lane B) shows that the bands in the LPS II region of SVQ293 migrate faster than those bands of HH103 (Figure 1, lane A). Differences are also evident in the LPS I region. Further studies have also shown that strain SVQ293 is a thiamine-requiring mutant and that its symbiotic nitrogen-fixation capacity with soybean plants is severely decreased (A. M. Buendía-Clavería and J. E. Ruiz-Sainz, unpublished work). The polysaccharide was extracted with hot phenol/water, treated with different enzymes and finally purified by gel-permeation chromatography. Two fractions were isolated. Monosaccharide analysis of the minor fraction revealed it to contain Man, GalA, Gal, Glc and Kdo; it thus had a very similar composition to that of the LPS in the wild-type *S. fredii* HH103 (results not shown). Monosaccharide analysis and ^{1}H-NMR showed that it also contained 3-hydroxytetradecanoic acid. Furthermore the SDS/PAGE profile (Figure 1, lane C) was characteristic of LPS. The polysaccharide in the minor fraction was therefore identified as the LPS of mutant SVQ 293. The major polysaccharide fraction, showing a quite distinct profile on SDS/PAGE (Figure 1, lane D), was subjected to the analyses described below.

Figure 1 SDS/PAGE of *S. fredii* HH103 (wild-type) and *S. fredii* SVQ293 (mutant) LPS

Lane A, *S. fredii* HH103 (wild-type) LPS; lane B, *S. fredii* SVQ293 (mutant) LPS; lane C, high-molecular-mass fraction obtained by gel-permeation chromatography of *S. fredii* SVQ293 polysaccharide; lane D, low-molecular-mass fraction obtained by gel-permeation chromatography of *S. fredii* SVQ293 polysaccharide.

Analysis of the polysaccharide

Monosaccharide composition

GLC–MS analysis of the trimethylsilylated methyl glycosides obtained on methanolysis and trimethylsilylation of the poly-

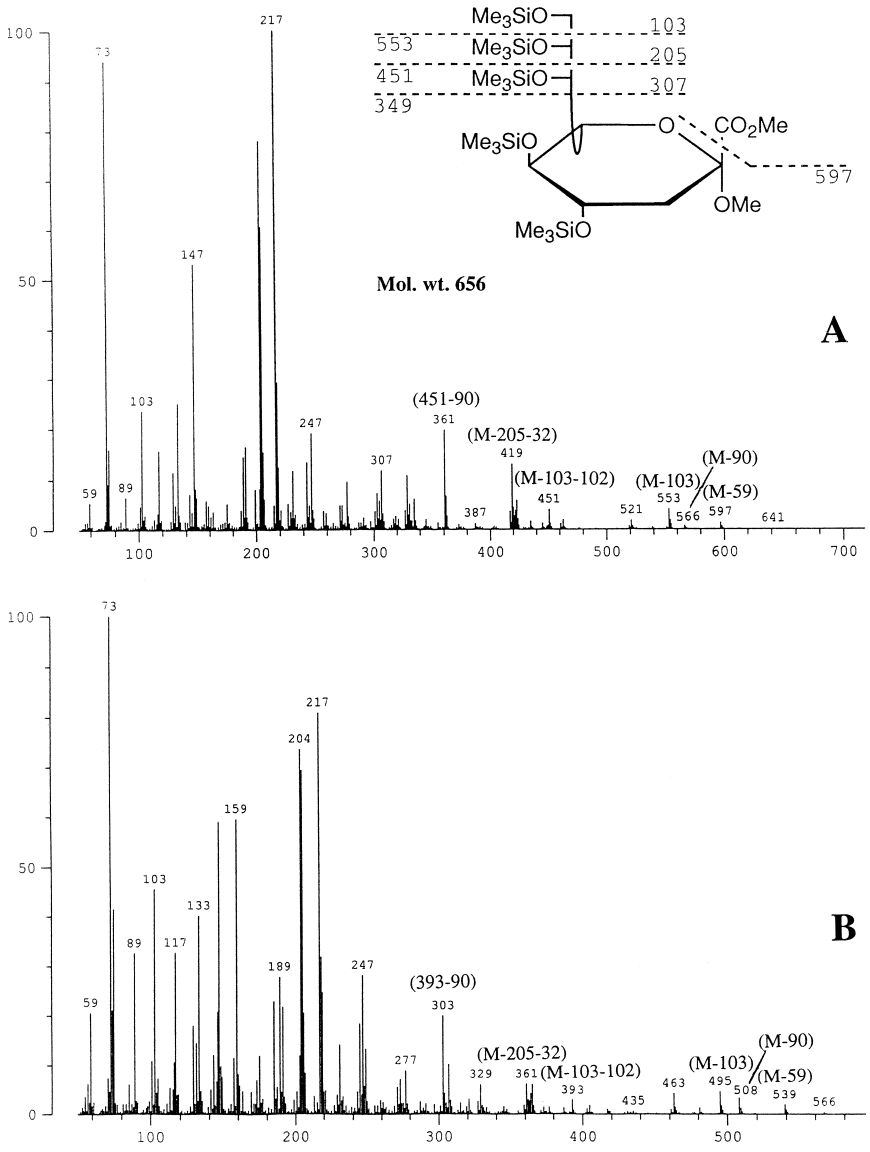

Figure 2 EI-MS and fragmentation schemes for trimethylsilylated methyl glycosides of Kdn (A) and the *O*-methyl-Kdn derivative (B)

saccharide revealed that it contains ribose, galactose, Kdn and a Kdn derivative in the molar ratios 1:1:0.25:0.75.The mass spectra of Kdn and the Kdn derivative are shown in Figure 2. We assign the structures of the different fragments on the basis of the fragmentation pattern proposed by Mononen [30]. The masses of the fragments arising from analogous cleavages of the two compounds show a difference of 58 mass units (*m/z* 597 and 539, 566 and 508, 553 and 495, 451 and 393, 419 and 361, 361 and 303). This difference can be explained by the presence of an *O*-methyl group in the trimethylsilyl ether of the Kdn derivative in place of a trimethylsilyl group in the trimethylsilyl ether of the Kdn. Furthermore the methyl group is located on position *O*-4 or *O*-5, because the fragments at *m/z* 103, 205 and 307, arising from the sequential cleavage of C-9–C-8, C-8–C-7 and C-7–C-6, are present in the mass spectra of both the Kdn and *O*-Me-Kdn.

Ribose and galactose were assigned as D-Rib and D-Gal after GLC–MS analysis of their trimethylsilylated 2-butyl glycosides prepared by using (+)-2-butanol and (±)-2-butanol.

Methylation analysis

The polysaccharide was methylated by the method of Ciucanu and Kerek [18] and then hydrolysed, reduced with NaB^2H_4 and acetylated. GLC–MS analysis of the resulting partly methylated alditol acetates showed the presence of 1,2,4-tri-*O*-acetyl-1-deutero-3,5-di-*O*-methylribitol derived from 2-linked ribofuranose, 1,2,5-tri-*O*-acetyl-1-deutero-3,4,6-tri-*O*-methylgalactitol from 2-linked galactopyranose, and 2,6,9-tri-*O*-acetyl-3-deoxy-2-deutero-5,7,8-tri-*O*-methyl-*glycero-galacto*-γ-nononolactone (Figure 3) from the γ-lactone of 9-linked-*O*-Me-Kdn in the pyranose ring.

NMR analysis

The chemical shifts for the ^1H and ^{13}C resonances of the polysaccharide were assigned from DQF-COSY, 1D-TOCSY and HSQC experiments (Table 1). The results of the ^1H–^{13}C heterocorrelation experiments (HSQC) are shown in Figure 4.

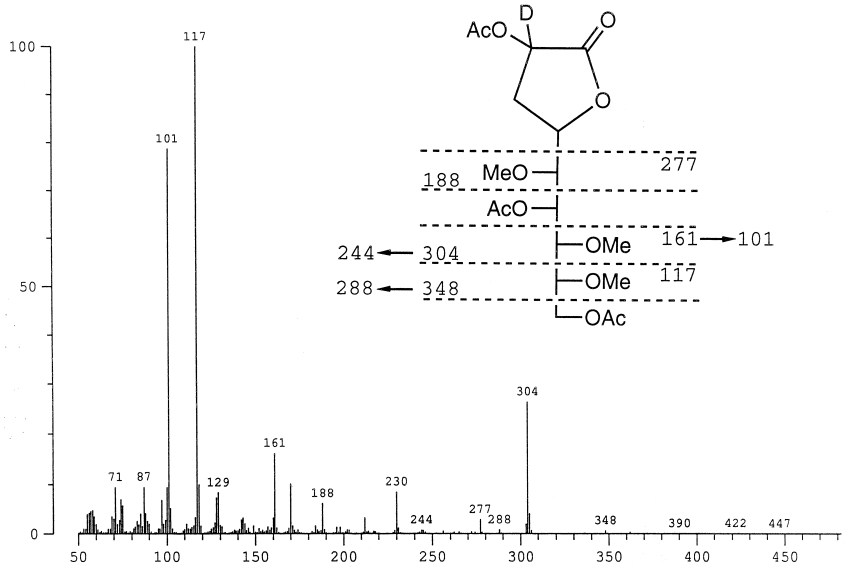

Figure 3 EI-MS and fragmentation scheme for 2,6,9-tri-*O*-acetyl-3-deoxy-2-deutero-5,7,8-tri-*O*-methyl-*glycero*-*galacto*-γ-nononolactone

Table 1 ^{1}H-NMR and ^{13}C-NMR chemical shifts, δ (p.p.m.), for the polysaccharide

Assignments with footnote symbols could be interchanged with others with the same symbol.

		Position									
Residue		1	2	3	4	5	6	7	8	9	Me
→ 2)-β-D-Rib*f*-(1 → (**a**)	H	5.20	4.13	4.36	4.08	3.82 (a) 3.66 (b)					
	C	105.0	79.0	70.5†	83.0	62.7					
→ 2)-α-D-Gal*p*-(1 → (**b**)	H	5.06	4.36	3.93	4.02	4.08	3.73 (a) 3.73 (b)				
	C	95.6	71.0*	67.7	69.3	71.1*	61.3				
→ 9)-α-D-5-*O*-Me-Kdn*p*-(2 → (**c**)	H	–	–	1.70 (ax) 2.74 (eq)	3.66	3.34	3.57	3.85	4.02	4.04 (a) 3.74 (b)	3.57
	C	172.9	99.2	40.2	70.2†	79.8	73.2	67.3	70.7	68.7	60.5

For the ribofuranose residue (unit **a**), the C-1 resonance is located at δ 105.0 p.p.m.; this fact and the low $J_{1,2}$ value (approx. 0 Hz) suggest that this residue is the β anomer (see below). Furthermore the downfield shift of C-2 (δ 79.0 p.p.m.) indicates that this position is substituted. For the galactopyranose residue (unit **b**), a cross-peak at δ 5.06 p.p.m. and δ 95.6 p.p.m. for H-1 and C-1 respectively was observed in this spectrum; this fact and the low $J_{1,2}$ value (approx. 0 Hz) show that this residue is the α anomer. Moreover the signal corresponding to C-2 is shifted downfield (δ 71.0 p.p.m.) from its expected value [31], indicating that position 2 in this unit is substituted. For the 5-*O*-Me-Kdn*p* residue (unit **c**) a δ H-3eq value of 2.74 p.p.m. was found. This value is characteristic of the α anomer [32]. Additionally, the downfield shifts observed for C-5 and C-9 resonances indicate that these positions are substituted [32]. The methylenic nature of C-5 (unit **a**), C-6 (unit **b**), C-3 (unit **c**), and C-9 (unit **c**) is unequivocally demonstrated by the negative sign (broken lines) of their one-bond proton–carbon correlation cross-peaks in this spectrum. Finally, a cross-peak at δ 3.57 p.p.m. (^{1}H) and δ 60.5 p.p.m. (^{13}C), characteristic of a methoxy group, is observed in the HSQC spectrum.

In addition, a 2D-NOESY was performed for the polysaccharide. The NOE connectivities observed are presented in Table 2. The inter-residue NOEs between H-1 (unit **a**) and H-9a,b (unit **c**); and connecting H-1 (unit **b**) with H-1 (unit **a**) and H-2 (unit **a**), allowed us to determine that the sequence of the residues in the polysaccharide is **b** → **a** → **c**. Finally, the intra-residue NOE observed between H-5 (unit **c**) and the MeO group suggests that the methyl group is located on *O*-5. These results allowed us to propose tentatively the following repeating unit for the polysaccharide: → 2)-α-D-Gal*p*-(1 → 2)-β-D-Rib*f*-(1 → 9)-α-5-*O*-Me-Kdn*p*-(2 → .

Analysis of the oligosaccharide repeating unit

To confirm these results, the oligosaccharide repeating unit was obtained on partial hydrolysis of the polysaccharide.

Partial hydrolysis and isolation

The polysaccharide was treated with water at 60 °C and allowed to autohydrolyse. The hydrolysate was chromatographed on

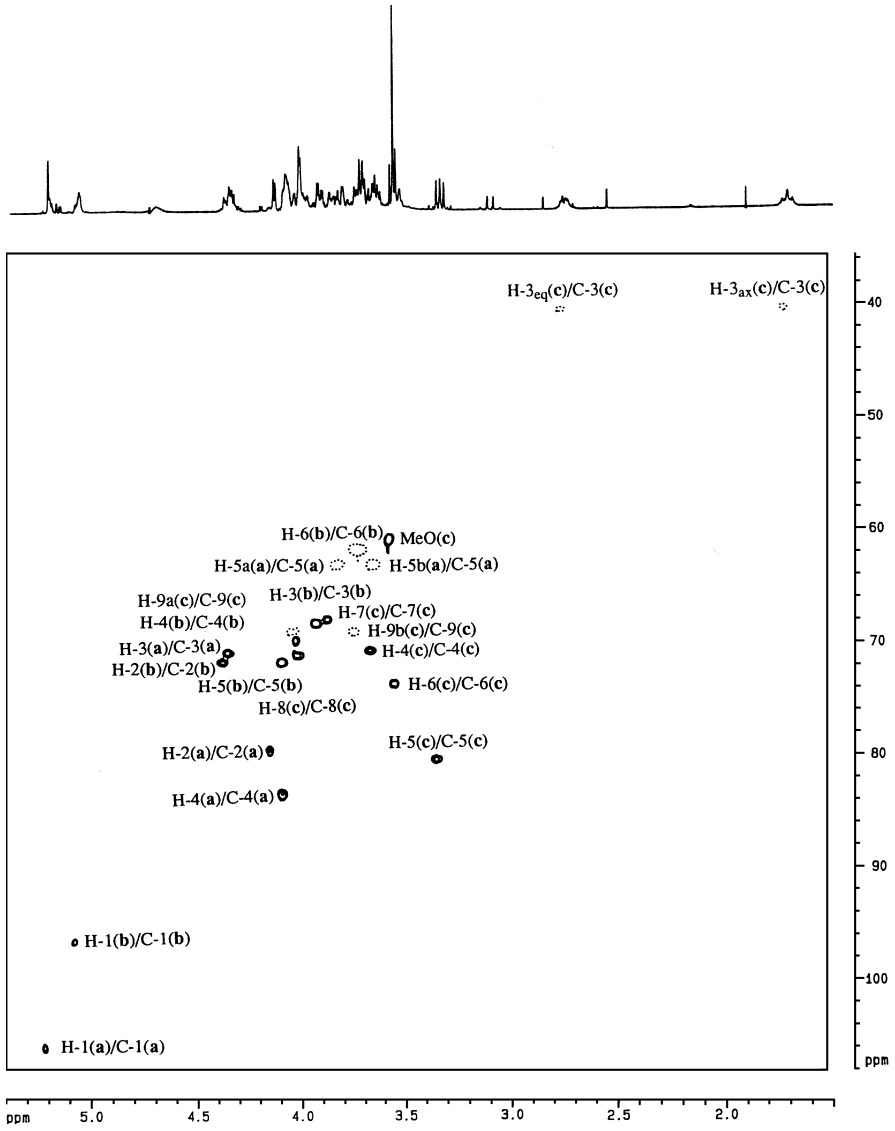

Figure 4 500 MHz ^{1}H-NMR and multiplicity-edited 2D-heteronuclear one-bond proton–carbon correlation experiment registered in the HSQC mode for the polysaccharide

Positive peaks (solid lines) correspond to methine and methyl carbons, whereas negative peaks (broken lines) correspond to methylenic carbons.

Sephadex G-50 and an oligosaccharide was isolated. GLC–MS analysis of the trimethylsylilated methyl glycosides shows that the oligosaccharide has the same composition as the polysaccharide.

FAB-MS and CID-MS

On positive-ion FAB-MS analysis, $[M+H]^+$, $[M+Na]^+$ and $[M+K]^+$ pseudomolecular ions were observed at m/z 577, 599 and 615, corresponding to a single trisaccharide of composition $Hex_1Pent_1Kdn_1Me_1$, where Hex and Pent are hexose and pentose residues respectively. Because the trisaccharide contains an acidic residue, negative-ion CID-MS was performed to determine the sequence of the trisaccharide and the residue to which the methyl group is attached. The spectrum that was obtained (Figure 5) contained a series of ions that could be rationalized as having arisen by charge-remote fragmentation, as shown in the fragmentation diagram. The ions observed allow the sequence of the trisaccharide (Hex-Pent-*O*-Me-Kdn) to be assigned. Interestingly they also allow further conclusions about the site of substitution of the methyl group to be drawn. The ion at m/z 87 shows that the methyl group is not borne on C-1, C-2 or C-3, whereas the ion at m/z 143 makes it clear that the methyl is attached via either C-4 or C-5. Mechanistically, it would be very difficult to rationalize the ion at m/z 143 as having arisen from a structure bearing a methoxy group on C-4, so that we conclude that C-5 bears a methoxy group. This sequence is the same as that deduced from the NMR studies of the polysaccharide.

Methylation analysis

The isolated trisaccharide was carbonyl-reduced with NaB^2H_4 and then alkylated with C^2H_3I to locate the methyl group present in the *O*-methyl-Kdn. The positive-ion FAB mass spectrum of the fully deuteromethylated trisaccharide alditol contained an $[M+Na]^+$ pseudomolecular ion at m/z 806; the EI-MS frag-

Table 2 NOE contacts observed for the polysaccharide

Inter-residue NOEs are shown in italics.

Residue	Proton	Correlation to
→ 2)-β-D-Rib*f*-(1 → (**a**)	H-1	4.13 (**a**,H-2); *5.06* (***b***,*H-1*); *4.04* (***c***,*H-9a*); *3.74* (***c***,*H-9b*)
	H-2	4.36 (**a**,H-3); *5.06* (***b***,*H-1*)
	H-4	3.82 (**a**,H-5a); 3.66 (**a**,H-5b)
	H-5a	3.66 (**a**,H-5b)
→ 2)-α-D-Gal*p*-(1 → (**b**)	H-1	4.36 (**b**,H-2); *5.20* (***a***,*H-1*); *4.13* (***a***,*H-2*)
	H-3	4.02 (**b**,H-4); 4.08 (**b**,H-5)
	H-5	3.73 (**b**,H-6a,b)
→ 9)-α-5-*O*-Me-Kdn*p*-(2 → (**c**)	H-3ax	2.74 (**c**,H-3eq); 3.34 (**c**,H-5)
	H-3eq	3.66 (**c**,H-4)
	H-5	3.57 (**c**,Me)
	H-7	3.57 (**c**,H-6 or Me)
	H-9a	3.74 (**c**,H-9b); *5.20* (***a***,*H-1*)
	H-9b	*5.20* (***a***,*H-1*)

mentation pattern and the structure are shown in Figure 6. The fragments at *m*/*z* 231 and 397 show that the monosaccharide sequence is Gal-Rib-*O*-Me-Kdn as deduced from the results of CID-MS analysis of the trisaccharide and NMR analysis of the polysaccharide. The fragments at *m*/*z* 171 and 215 demonstrate that the *O*-methyl group is on C-5. Finally, the fragment at *m*/*z* 474 is consistent with the Rib*f*-5-*O*-methyl-Kdn linkage being (1 → 9). The fully deuteromethylated trisaccharide alditol was then further hydrolysed, reduced with NaB^2H_4 and acetylated. GLC–MS analysis of the resulting monosaccharide derivatives showed the presence of 1,5-di-*O*-acetyl-1-deutero-2,3,4,6-tetra-*O*-trideuteromethylgalactitol from the non-reducing Gal*p*, 1,2,4-tri-*O*-acetyl-1-deutero-3,5-di-*O*-trideuteromethylribitol from 2-linked Rib*f*, and 1,9-di-*O*-acetyl-3-deoxy-1,1,2-trideutero-2,4,6,7,8-penta-*O*-trideuteromethyl-5-*O*-methyl-*glycero*-*galacto*-nonitol (Figure 7) derived from 9-linked 5-*O*-methyl-Kdn pyranose.

NMR analysis

The chemical shifts for the ^1H and ^{13}C resonances of the trisaccharide were assigned from DBF-COSY, 1D-TOCSY and HSQC experiments (Table 3). The ^1H-NMR spectrum is shown in Figure 8(a). From the data for the polysaccharide, the high δ value of C-1 of the ribofuranose residue (δ 105.8 p.p.m.) suggests a β anomer. This supposition is confirmed by the *J* coupling pattern found for all the protons of the residue (see Table 3) characteristic of a β-D-Rib*f* in $^3T_2$ conformation [33]. For the galactopyranose residue, we observed a drastic change in the chemical shifts for C-2 and H-2, which appear at higher field, consistent with loss of the *O*-2 substituent. The δ value for the H-3eq of the 5-*O*-Me-Kdn*p* residue is at 2.11 p.p.m., which is characteristic of a β anomer, the major anomer in the non-linked Kdn residue [34]. These results confirm that the Rib*f* is present as the β anomer and demonstrate that the trisaccharide arises from the selective cleavage of the α-5-*O*-Me-Kdn*p*-(2 → 2)-α-D-Gal*p* linkage.

Finally, the 1D-TOCSY experiment shown in Figure 8(b) permits the detection of the signal for H-5 of a minor non-methylated Kdn component, indicating that not all the Kdn residues are 5-*O*-methylated; this is consistent with the results of the monosaccharide analyses of the polysaccharide and the trisaccharide and allows us to confirm the ratio of methylated to non-methylated Kdn. The TOCSY spectrum was obtained by selective excitation of the Kdn H-3ax. The δ value at 3.54 p.p.m. arising from H-5 in the non-methylated Kdn component is very close to the published value [34,35], whereas the same signal for

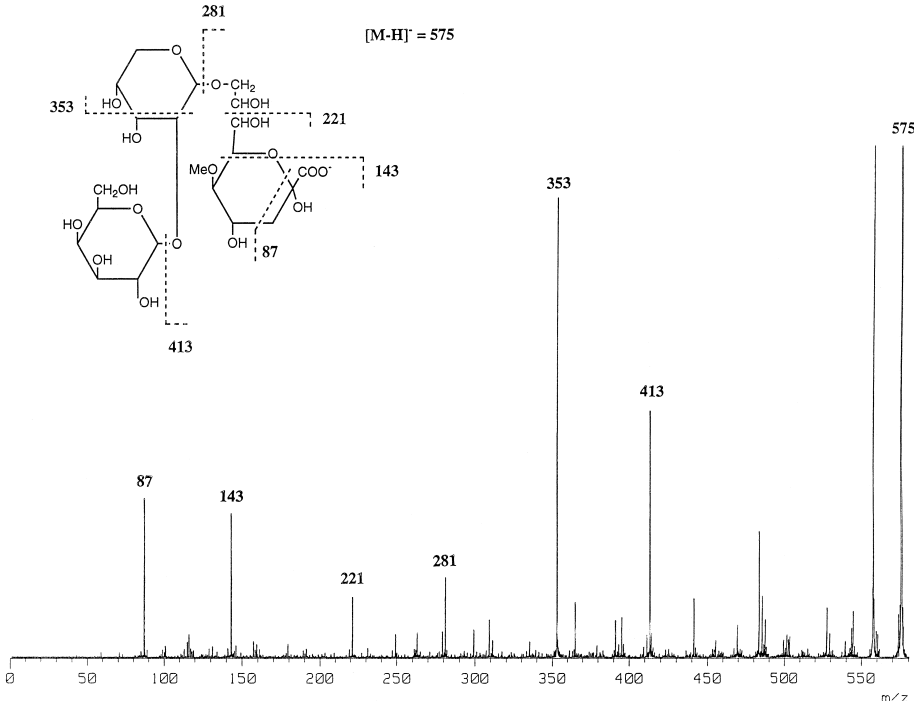

Figure 5 CID-MS of the [M-H]⁻ at *m*/*z* 575 and fragmentation scheme for the trisaccharide

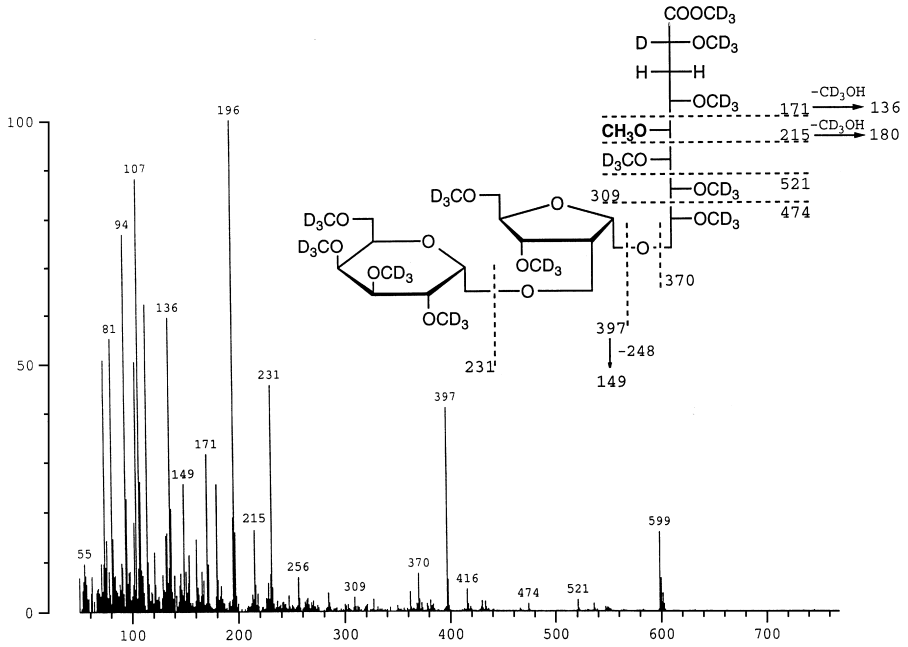

Figure 6 EI-MS and fragmentation pattern for fully methylated trisaccharide alditol of the trisaccharide

The ion at *m/z* 599 corresponds to a baldJ$_1$ ion type.

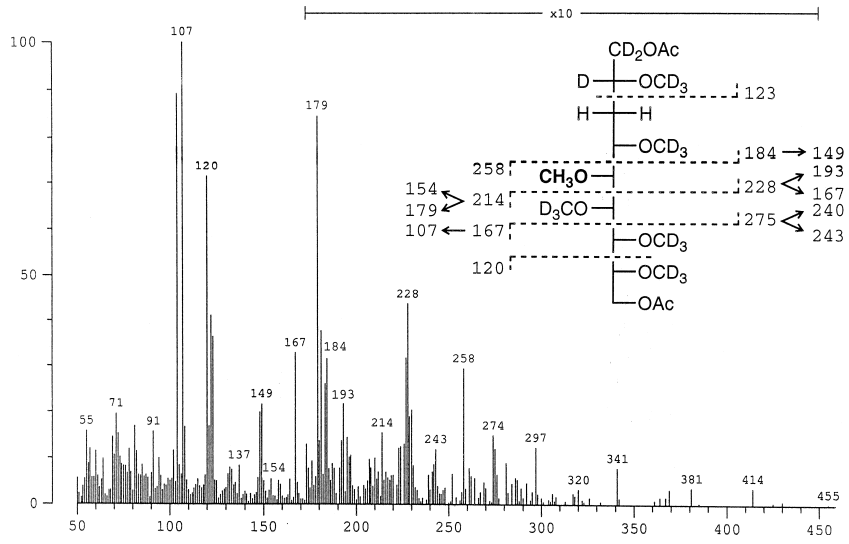

Figure 7 EI-MS for 1,9-di-*O*-acetyl-3-deoxy-1,1,2-trideutero-5-*O*-methyl-2,4,6,7,8-penta-*O*-trideuteromethyl-*glycero*-*galacto*-nonitol

this proton in the major component (5-*O*-Me-Kdn*p*) is located at δ 3.30 p.p.m.

On the basis of these results we conclude that the trisaccharide has the structure shown in Figure 9, which is consistent with the structure of the polysaccharide proposed above.

DISCUSSION

The results of this study show the presence of a Kdn-rich polysaccharide in the crude polysaccharide extract of *S. fredii* SVQ293. This strain was obtained by random transposon Tn5-Mob mutagenesis of *S. fredii* HH103 with the suicide plasmid pSUP5011. This mutant forms a colony that produces more slime than its parental strain; it is a thiamine-requiring mutant and its symbiotic nitrogen-fixation capacity with soybean plants is severely decreased (A. M. Buendía-Clavería and J. E. Ruiz-Sainz, unpublished work). The cell-associated polysaccharides were extracted by the hot phenol/water method, followed by treatment with enzymes and gel-permeation chromatography on Sephacryl S-500. Two fractions with different molecular masses were isolated. The higher-molecular-mass fraction contains the minor component and has a typical LPS profile on silver-stained SDS/PAGE (Figure 1, lane C). This profile, and the presence of a fatty acid and Kdo in its GLC–MS analysis, indicate that this

Table 3 ^{1}H-NMR and ^{13}C-NMR chemical shifts, δ (p.p.m.) and coupling constants, *J* (Hz), for the trisaccharide

Assignments with an asterisk could be interchanged.

Residue		Position 1	2	3	4	5	6	7	8	9	Me
→ 2)-β-D-Rib*f*-(1 → (**a**)	H	5.13	4.16	4.31	4.05	3.78 (a) 3.61 (b)					
	J	(*1,2*) 1.0	(*2,3*) 4.8	(*3,4*) 6.9	(*4,5a*) 2.8	(*4,5b*) 6.0	(*5a,5b*) −12.3				
	C	105.8	78.9	70.7	83.4	62.8					
α-D-Gal*p*-(1 → (**b**)	H	5.12	3.81	3.91	3.95	4.07	3.70 (a) 3.69 (b)				
	J	(*1,2*) 3.9	(*2,3*) 10.3	(*3,4*) 3.4	(*4,5*) 1.0	(*5,6a*) 4.8	(*5,6b*) 7.0	(*6a,6b*) −10.5			
	C	97.7	68.6	69.3	69.6*	71.7	61.7				
→ 9)-β-5-*O*-Me-Kdn*p* (**c**)	H	–	–	1.73 (ax) 2.11 (eq)	3.98	3.30	3.85	3.71	3.82	3.97 (a) 3.64 (b)	3.54
	J	(*3ax,4*) 12.4	(*3eq,4*) 5.0	(*3ax,3eq*) −12.5	(*4,5*) 9.5	(*5,6*) 9.9	(*6,7*) 2.5	(*7,8*) 8.9	(*8,9a*) 2.3	(*8,9b*) 5.6	(*9a,9b*) −10.7
	C	177.2	96.8	39.8	69.6*	80.9	70.9	68.6	69.7*	70.3	60.7

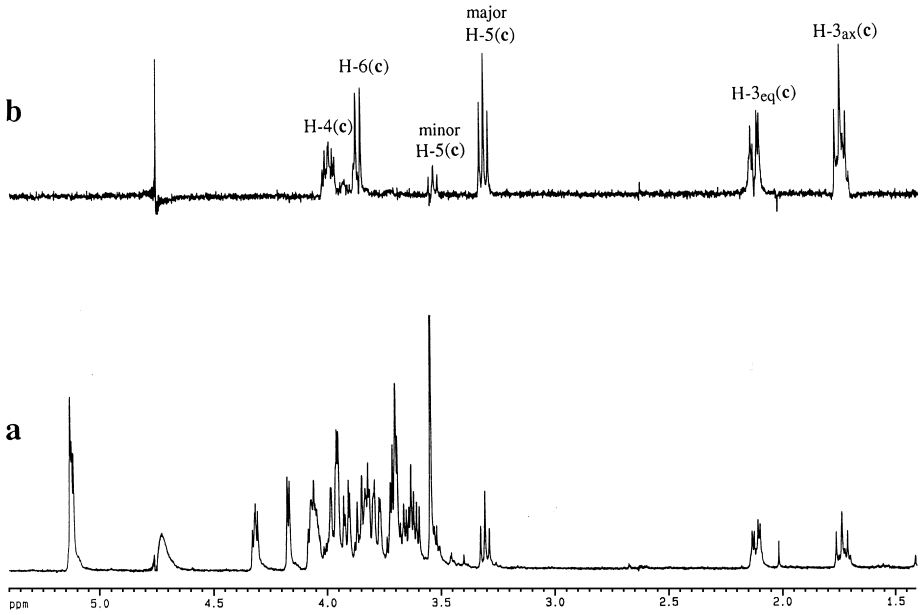

Figure 8 ^{1}H-NMR spectrum at 500 MHz (a) and 1D-TOCSY subspectrum (b) obtained by selective excitation of the signal at δ 1.73 ppm for the trisaccharide

The signal at δ 3.54 p.p.m. is assigned to H-5 of the minor component of the trisaccharide (non-5-*O*-methylated Kdn) and the signal at δ 3.30 p.p.m. is assigned to H-5 of the major component of the trisaccharide (5-*O*-methylated Kdn). Signals for H-3ax, H-3eq, H-4 and H-6 corresponding to the major component are also indicated.

polysaccharide is an LPS. In addition, its monosaccharide analysis and SDS/PAGE profile are similar to those of the parental strain (Figure 1, lane A). The lower-molecular-mass fraction contains the major component; its SDS/PAGE profile (Figure 1, lane D) and the absence of fatty acids and Kdo indicate that this polysaccharide is a separate and structurally distinct type of polysaccharide that has not been previously identified in rhizobial species.

Monosaccharide analysis showed that the polysaccharide contains ribose, galactose, Kdn and 5-*O*-Me-Kdn. The presence of a methyl group as a substituent of Kdn was deduced from the EI-MS spectrum of its trimethylsilylated derivative. The location of the methyl group was suspected from the fragments in the EI and CID-MS spectra, which show that positions *O*-4 and *O*-5 are the only possible substitution points. On methylation analysis the generation of a γ-lactone (at C-4) instead of the more stable δ-lactone (at C-5) indicates that the OH at C-5 was previously methylated. From the 1D-NMR and 2D-NMR experiments we obtained the individual ^{1}H and ^{13}C resonances that demonstrate the linkage between the different sugar units and the anomericity for Gal and 5-*O*-Me-Kdn. The Rib was tentatively assigned as the β anomer. From NOESY experiments, the sequence and the substitution of the methyl group at the OH on C-5 were deduced. To confirm the above results, a trisaccharide was isolated and its structure was determined unequivocally. From the CID-MS of the trisaccharide, the EI-MS analysis of the per-*O*-alkylated

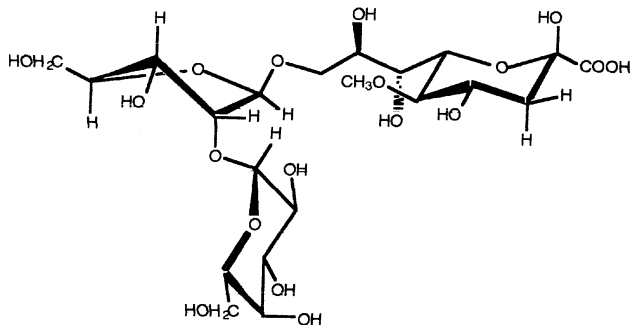

Figure 9 Structure of the trisaccharide isolated by partial hydrolysis of the Kdn-containing polysaccharide

trisaccharide alditol and from the methylation analysis, the sequence proposed and the anomericity of the Rib deduced from the NMR results were confirmed. The structure of a new type of cell-associated polysaccharide containing 5-*O*-Me-Kdn has thus been determined in a rhizobial strain.

The Kdo-rich polysaccharide found in the wild-type strain HH103-1 yields a ^{1}H-NMR spectrum (M. A. Rodríguez-Carvajal and A. M. Gil-Serrano, unpublished work) that is very similar to that reported for an analogous preparation from *R. meliloti* AK631 [6]. Apparently, this Kdo-rich polysaccharide from strain HH103-1 is replaced by the Kdn-rich polysaccharide in mutant strain SVQ293. We believe that this shift in bacterial polysaccharide production is likely to be due to a pleiotropic effect of the auxotrophic mutation. In *R. meliloti* strain SU47, *exo* mutations result in the development of nodules that do not contain bacteria and therefore fail to fix nitrogen (Fix$^-$) [36]. In contrast, *R. meliloti* 41 mutants with mutations in *exo* genes are Fix$^+$. Petrovics et al. [37] have shown that in *R. meliloti* strain 41 the Kdo-rich polysaccharide compensates for *exo* mutations during symbiotic nodule development, providing equivalent information for the host plant during this development.

Mutant SVQ293 produces a Kdn-rich polysaccharide instead of the typical Kdo-rich polysaccharide. The mutant also shows alterations in its nodulation host range (A. M. Buendía-Clavería and J. E. Ruiz-Sainz, unpublished work). Experiments aimed at determining the symbiotic significance of the Kdn-rich polysaccharide should provide valuable information on the differential roles of the bacterial polysaccharides during the nodulation process.

We thank the Comisión Interministerial de Ciencia y Tecnología (grant no. BIO096-1469-C03-01 and 02) and the Netherlands Organisation for Scientific Research (J.T.-O.) for financial support.

Received 19 March 1998/1 June 1998; accepted 30 June 1998

REFERENCES

1 Van Rhijn, P. and Vanderleyden, J. (1995) Microbiol. Rev. **59**, 124–142
2 Spaink, H. P. (1995) Annu. Rev. Phytopathol. **33**, 345–368
3 Pueppke, S. G. (1996) Crit. Rev. Biotechnol. **16**, 1–51
4 Gray, J. W., de Maagd, R. A., Rolfe, B. G., Johnston, A. W. and Lugtenberg, B. J. (1992) Molecular Signals in Plant–Microbe Communications (Verma, D. V. S., ed.), pp. 359–376, CRC Press, Boca Raton, FL
5 Reuber, T. L. and Walker, G. C. (1993) Cell **74**, 269–280
6 Reuhs, B. L., Carlson, R. W. and Kim, J. S. (1993) J. Biol. Chem. **175**, 3570–3580
7 Jann, B. and Jann, K. (1990) Curr. Top. Microbiol. Inmunol. **150**, 19–42
8 Beringer, J. E. (1974) J. Gen. Microbiol. **84**, 188–198
9 Maniatis, T., Fritsch, E. F. and Sambrook, J. (1982) Molecular Cloning: A Laboratory Manual, Cold Spring Harbor Laboratory, Cold Spring Harbor, NY
10 Simon, R. (1984) Mol. Gen. Genet. **196**, 413–420
11 Westphal, O. and Jann, K. (1965) Methods Carbohydr. Chem. **5**, 83–91
12 François, C., Marshall, R. D. and Neuberger, A. (1962) Biochem. J. **83**, 335–337
13 Köplin, R., Wang, G., Hötte, B., Priefer, U. B. and Pühler, A. (1993) J. Bacteriol. **175**, 7786–7792
14 Lesse, A. J., Campagnari, A. A., Bittner, W. E. and Apicella, M. A. (1990) J. Immunol. Methods **126**, 109–117
15 Kittelberger, R. and Hilbink, F. (1993) J. Biochem. Biophys. Methods **26**, 81–86
16 Chaplin, M. F. (1982) Anal. Biochem. **123**, 336–341
17 Gerwig, G. J., Kamerling, J. P. and Vliegenthart, J. F. G. (1978) Carbohydr. Res. **62**, 349–357
18 Ciucanu, I. and Kerec, F. (1984) Carbohydr. Res. **131**, 209–217
19 Blakeney, A. B., Harris, P. J., Henry, R. J. and Stone, B. A. (1983) Carbohydr. Res. **113**, 291–299
20 Waeghe, T. J., Darvill, A. G., McNeil, M. and Albersheim, P. (1983) Carbohydr. Res. **123**, 281–304
21 States, D. J., Haberkorn, R. A. and Ruben, D. J. (1982) J. Magn. Reson. **48**, 286–292
22 Bodenhausen, G. and Ruben, D. J. (1980) Chem. Phys. Lett. **69**, 185–189
23 Parella, T., Sánchez-Ferrando, F. and Virgili, A. (1997) J. Magn. Reson. **126**, 274–277
24 Boudot, D., Canet, D., Brondeau, J. and Bouble, J. C. (1989) J. Magn. Reson. **83**, 428–433
25 Boudot, D., Roumestand, C., To, F. and Canet, D. (1990) J. Magn. Reson. **90**, 221–227
26 Kupce, E. and Freeman, R. (1995) J. Magn. Reson. A **106**, 168–181
27 Roumenstand, C., Canet, D., Mahieu, N. and Toma, T. (1994) J. Magn. Reson. A **106**, 168–181
28 Carlson, R. W. (1984) J. Bacteriol. **158**, 1012–1017
29 Carlson, R. W. and Bhagyalakshmi, S. K. (1992) Carbohydr. Res. **231**, 205–219
30 Mononen, Y. (1981) Carbohydr. Res. **88**, 39–50
31 Bock, K., Pedersen, C. and Pedersen, H. (1984) Adv. Carbohydr. Chem. Biochem. **42**, 193–225
32 Strecker, G., Wieruszeski, J. M., Michalski, J. C. and Montreuil, J. (1992) Biochem. J. **287**, 905–909
33 Angyal, S. J. (1979) Carbohydr. Res. **77**, 37–50
34 Iwasaki, M., Inone, S. and Troy, F. A. (1990) J. Biol. Chem. **265**, 2596–2602
35 Knirel, Y. A., Kocharova, N. A., Shaskov, A. S., Kochetkov, N. K., Mamontova, V. A. and Soloveva, T. F. (1989) Carbohydr. Res. **188**, 145–155
36 Leigh, J. A., Signer, E. R. and Walker, G. C. (1985) Proc. Natl. Acad. Sci. U.S.A. **82**, 6231–6235
37 Petrovics, G., Putnoky, P., Reuhs, B., Kim, J., Thorp, T. A., Noel, K. D., Carlson, R. W. and Kondorosi, A. (1993) Mol. Microbiol. **8**, 1083–1094